

# Characteristics of DC Corona Streamers Induced by UV Laser Irradiation in Non-Thermal Plasma

T. Ohkubo, S. Kanazawa, Y. Nomoto, M. Kocik<sup>1</sup>, and J. Mizeraczyk<sup>1</sup>

Department of Electrical and Electronic Engineering, Oita University, 700 Dannoharu, Oita 870-1192, Japan

<sup>1</sup>Centre for Plasma and Laser Engineering, Institute of Fluid Flow Machinery, Polish Academy of Sciences, Fizyka 14, 80-231 Gdańsk, Poland

---

**Abstract:** Positive corona streamers are widely used in the field of air pollution control such as NO<sub>x</sub> or SO<sub>x</sub> removal and VOCs decomposition based on non-thermal plasma chemical process. In this study, the characteristics of DC positive corona streamers induced by UV laser irradiation are investigated in the tube-to-plane electrode configuration with electrode gap spacing of 3 cm. The streamer images were recorded using an ICCD camera with a nanosecond order time resolution. During the DC corona discharge, regular streamers appear with tens of ms intervals, the duration of which considerably fluctuates. This makes time resolved streamer observation by the ICCD camera extremely difficult. However, additional streamers with a predictable inception time can be induced by UV laser irradiation. As a result, the current waveform characteristics of the laser-induced streamers were obtained. In this work, three-dimensional streamer structures including the streamer propagation and branching were studied. Also the streamer propagation velocity was evaluated.

---

## Introduction

The research of the corona discharge has a long history over 100-years (1-5). The corona discharges have the form of avalanches, bursts, burst pulses, glows, primary streamers, and secondary streamers (3). The mode of the corona discharge depends on the electrode configuration, applied voltage, working gas, etc. Especially, the positive corona streamers became of interest in recent years because of their potential to be utilized in new technologies for the plasma-chemical treatment of gases and liquids (for example, removal of NO<sub>x</sub> and SO<sub>x</sub> from flue gases, destruction of hazardous gaseous pollutants, and conversion of hydrocarbons) (6-12). A detail understanding of the streamers is important not only for improving the efficiency of gas treatment but also supplying the advanced data concerning to the corona discharge. Up to now, it is known that the positive corona streamers consist of the ionization region formed by the space charge of positive ions (called the 'streamer head'), propagating through the ambient gas towards the cathode, and the quasi-neutral channel (called the 'streamer channel'), which is formed on the track passed by the streamer head. The streamer head, difficult to be observed, is considered to be a disk of a diameter and thickness of 200 μm and 20 μm, respectively (13-15). The streamer head velocity is 10<sup>5</sup>-10<sup>6</sup> m/s (15-17). In spite

of these understandings, the insufficient understanding of corona discharge process for the gas treatment is due to the complexity of physical and chemical phenomena, which occur in the spatially and temporally complex plasma of corona discharges. These phenomena could not be studied with the required spatial and temporal resolution due to the lack of the appropriate equipment. However, recent progress in the development of an intensifier-gated charge-coupled device (ICCD) camera, imaging spectrographs and fast digital image processing has made the investigation of the filamentary discharges, including the corona discharges, possible with higher sensitivity and spatial and temporal resolution than ever.

For the temporally resolved imaging of corona discharges, the synchronization of the discharge pulse and the opening of the ICCD camera (gate start and exposure time) is a crucial point. The DC corona discharge consists of regular self-repetitive current pulses with pulse duration up to several hundred nanoseconds and repetition frequency in the range of 1 to 100 kHz depending on the electrode configuration, gas composition, etc. However, the time interval between the current pulses of the DC corona streamers usually fluctuates. In order to perform time resolved imaging of the transient discharge (e.g. corona discharge), a reference time must be assigned to the characteristic event related to the discharge, e.g. related to the inception of the current pulse. This reference time is required to establish the delay of the imaging (the moment of opening of the ICCD camera) with respect to the characteristic event, and

---

Keywords: DC positive corona discharge, regular corona streamer, streamer structure, laser-induced streamer

then to be able to trace the time evolution of the discharge during the exposure time of the ICCD camera. To perform time resolved observation of the streamers, the procedure consists of repeated image acquisition with the incremented delay between consecutive acquisitions. Such a procedure of scanning the time delay between the event and the image is known as the Boxcar scanning. Using the Boxcar scanning, the time evolution of the discharge can be revealed. In recent years, using the Boxcar scanning the spatial and temporal visualization of the pulsed corona streamers was carried out with a help of modern high sensitive and nanosecond-fast ICCD cameras (10, 15, 17-21).

In this study, we deal with DC streamers which are used as the non-thermal plasma for pollution control technology. A tube-to-plane electrode with electrode gap spacing of 3 cm is used. The inception of the corona current pulse is commonly accepted as the most convenient characteristic event for the measurement in both DC and pulsed coronas. However, as mentioned above, the inception of the DC corona current pulse is an uncontrolled stochastic process (due to the inception time delay fluctuation), while the inception of the pulsed corona is more or less controlled by the pulsed power supply. This makes the synchronization of Boxcar scanning easier in the case of the pulsed coronas. To overcome this problem in the case of DC coronas, a technique for the controlled inception of a DC corona pulse by an UV laser beam was developed (22-25). The discharge current of DC positive corona streamers consists of a train of pulsed discharge waveforms with a relative high repetition rate. When an UV laser beam pulse is shot between the electrodes, an additional corona current pulse is induced. The probability of coincidence of regular streamers and the laser beam pulse is quite low. Since the time controlled laser-induced streamer is also suitable to investigate the behavior of radicals with short lifetime (less than 1 ms) in DC coronas using laser-induced fluorescence (LIF) technique, we compared the properties of the laser-induced streamers to the regular streamers in order to confirm whether the laser-induced streamers were representative for the regular streamers. DC positive corona streamers induced by UV laser irradiation was observed using an ICCD camera. The streamer structure of the laser-induced streamers was investigated with respect to spatial and temporal aspects. Although there have been an experiments on laser-induced streamer using a YAG laser beam (26), the object of investigation was different from the research presented in this paper.

## Experimental Setup

Figure 1 shows the schematic diagram of the apparatus used in this study. DC positive corona streamers were generated in the tube-to-plane electrode configuration in air at atmospheric pressure. A stainless-steel pipe with a tube (1.0 mm in inner diameter, 1.5 mm in outer diameter) was used as the tube electrode. Two types of the plane electrodes were used: a perforated plate (100 mm in diameter) with holes of 1.5 mm in diameter and a stainless-steel 30 mesh plate (150 mm in diameter). The electrode gap spacing was constant and equal to 3 cm. DC high voltage with positive polarity was applied through a 10 M $\Omega$  resistor to the tube electrode. Two-dimensional images of regular and laser-induced DC corona streamers were recorded by an ICCD camera (LaVision, Flame Star II). The ICCD had an image size of 384 (V) x 576 (H) pixels and has the spectral sensitivity in the range of 200-800 nm. The streamer structure was investigated from the different view points such as "side view" (observation direction perpendicular to the laser beam propagation axis), "front view" (observation direction almost parallel to the laser beam propagation axis) and "bottom view" (through the mesh electrode, perpendicular to the laser beam propagation axis). In order to generate the laser-induced streamers, two lasers, a KrF excimer laser ( $\lambda = 248$  nm, pulse energy: 200 mJ) and a dye laser with SHG ( $\lambda = 281$  nm, pulse energy: 2 mJ), were used. A comparison between the streamers induced by the laser beam of different UV wavelength was made. In both cases the laser pulse duration was 20 ns. To check the influence of the laser beam properties on the generation of the laser-induced streamers, several laser beam geometries were used for the generation of laser-induced streamers, including cylindrical laser beam, focused laser beam and the so-called laser sheet (placed vertically or horizontally relative to the plane electrode). Also the location of the laser beam in the discharge gap was varied.

In order to take an image of the time-resolved streamer propagation in the gap, precise setting of the timing between the streamer inception and the opening of ICCD camera is a crucial. Figure 2 shows the definitions of parameters for observing the laser-induced streamer: time delay between the laser trigger signal and the laser pulse (L), laser-induced streamer inception (S) and gate opening (D) of the ICCD camera. The time delay D includes an additional delay (called an 'offset') caused by the controlling electronics, laser electronics, cables, etc. It was experimentally found that the offset time

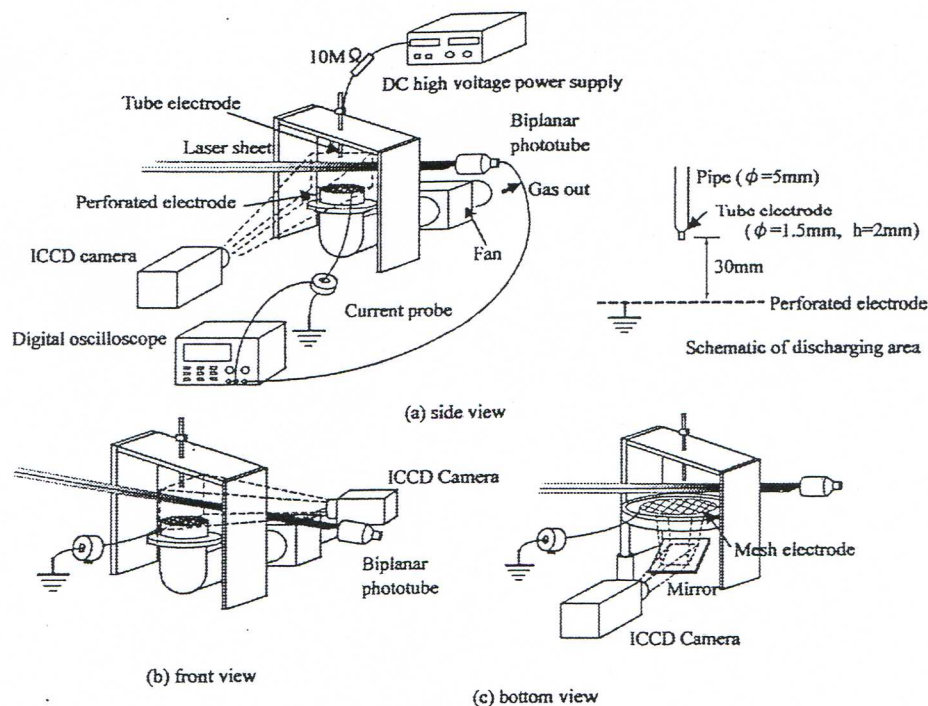


Figure 1. Setup with an ICCD camera for observation of the DC positive corona streamers.

is constant and equal to 55 ns. The laser pulse was monitored using a fast biplanar phototube (Hamamatsu, R1193U-55). The streamer current pulse was measured using a current probe (Pearson Electronics, Inc., Model 2878). The time relationship between the trigger signal, laser pulse and streamer current was measured by using a fast digital oscilloscope (HP Infinium, 1.5 GHz, 8 GSa/s). Hence, knowing precisely the timing of the laser pulse, current characteristic of streamers and gate opening time of the ICCD camera, it was possible to determine the phase of streamer evolution (D-S, time elapse from the start of streamer). The moment of opening of the ICCD camera and its exposure time were controlled independently by setting the "Delay time" and "Gate time" of the ICCD controller (resolution of 1 ns, minimum gate time of 5 ns).

### Results and Discussion

Figure 3 shows the comparison of the streamer images and the corresponding current waveform of the single DC regular and single laser ( $\lambda = 281$  nm, pulse energy: 2 mJ) induced streamers. The laser sheet (3 mm-thick and 25 mm-height) vertical relative to the plane electrode was placed between the electrodes. In Figure 5, one pixel size of the ICCD camera corresponds to 85  $\mu\text{m}$  in the image. Many branches are observed at an applied voltage (26 kV) typical of gas treatment. Besides, the outward-

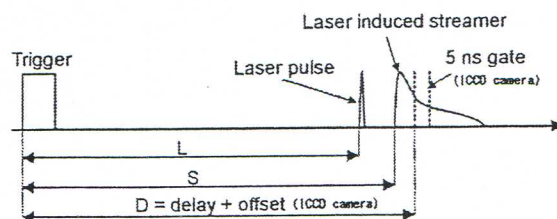
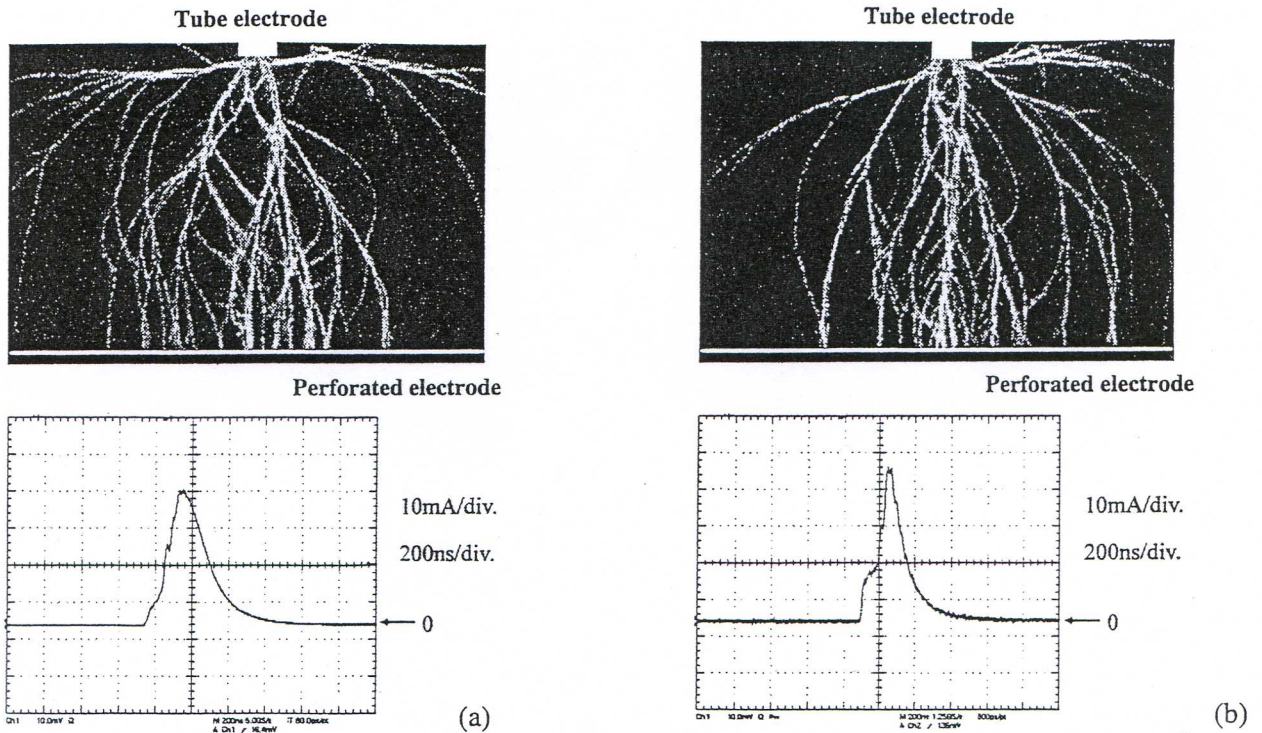


Figure 2. Timing between trigger signal for laser oscillation, laser pulse, laser-induced streamer current and ICCD gate width.

directed streamers did not bridge the entire gap and disappeared on the way to the grounded electrode. The branching phenomenon is considered to be due to electrostatic repulsion of the streamer head (15).

For a better understanding of the streamer structure such as a streamer diameter, Figure 4 shows the streamer image in the vicinity of the tube electrode. The streamers were generated from several points on the tube edge and propagated toward the grounded electrode with branching as shown in Figure 4. In Figure 4, one pixel size of the ICCD camera corresponds to 25  $\mu\text{m}$  in the image. The diameter of the streamer before branching is about 100-200  $\mu\text{m}$ .

In order to investigate the influence of the laser irradiation on the streamer structure, the comparison of the images of KrF excimer laser ( $\lambda = 248$  nm, pulse energy: 200 mJ) induced streamers taken from the different view points relative to the laser sheet direction is shown in Figure 5. The laser sheet



**Figure 3.** The images and corresponding current waveform of (a) the single regular DC corona streamer and (b) UV laser (281 nm)-induced streamer. Gate time of ICCD camera: 200  $\mu$ s. Gain of ICCD camera: 7. Applied voltage: 26 kV. Time division: 200 ns, current division: 10 mA.

(3 mm-thick and 20 mm-height) vertical relative to the plane electrode was placed between the electrodes. Figure 5(a) and (b) show the typical images ('side view' and 'front view') which were captured perpendicularly and almost parallel to the laser sheet direction, respectively. The image of streamers taken from the 'bottom side' is shown in Figure 5(c). From these images of the streamers, the influence of the laser irradiation on the streamer structure is negligible.

Although there are a considerable image-to-image variation in the appearance of the streamer discharge such as the trajectory of the streamer head and branching, the fundamental features of the laser-induced streamers are similar to those of the regular streamers. From the statistical point of view, no apparent difference between the regular and laser-induced streamers, in terms of the current pulse (i.e., rise time, width, amplitude), number of streamers, streamer diameter, branching distance and its angle, was observed by comparing the both images observed at the fixed experimental condition. Thus, the laser-induced streamers are representative for the regular DC corona streamers. Moreover, we found that the influence of the laser wavelength (248 nm and 281 nm, both of which are used for OH radical measurement by LIF (27-28)) and beam energy (in the range used in this experiment) on the generation

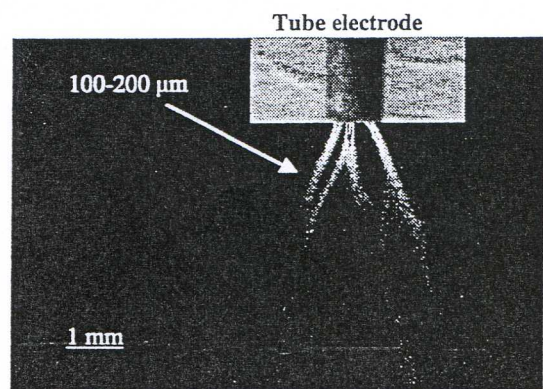


**Figure 4.** Streamers near the tube electrode at 25 kV. Gate time of ICCD camera: 200  $\mu$ s. Gain of ICCD camera: 5.5.

probability and streamer structure is negligible. However, the focused laser beam was found to be less efficient in the streamers generation compared to the cylindrical laser beam and vertical or horizontal laser sheet.

On the other hand, the streamer images are influenced by the experimental conditions such as the high voltage excitation mode (DC, or pulse), electrode configuration, and gas composition (15, 17, 18, 29). As the distance between the top of the laser sheet and the tip of the tube electrode increases, the time delay for streamer inception increases and the streamer triggering probability decreases (30).

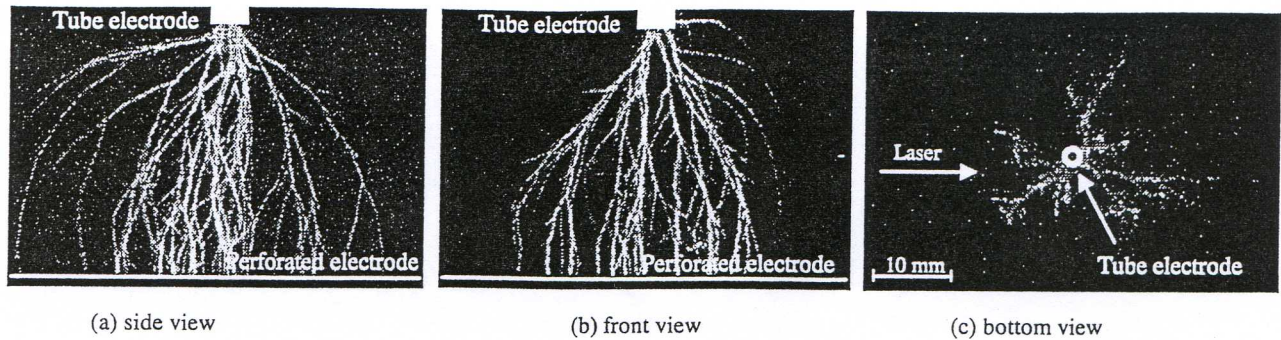


**Figure 5.** The images of the KrF laser (248 nm) -induced streamers from the different points of view; (a) side view, (b) front view, and (c) bottom view. The circle with the diameter of 3.5 cm, dotted line in (c) indicates the streamer propagating area. Gate time of ICCD camera: 400 ns. Gain of ICCD camera: 7. Applied voltage: 26 kV.

Since the corona discharge pulse is to some extent a stochastic phenomenon, the distribution of the time delay between the laser pulse and laser-induced streamer appearance was investigated prior to the time resolved streamer observation. Figure 6 shows the distribution of the time delay (S-L in Figure 2) of UV laser (281 nm)-induced streamer in respect to the laser pulse. The laser-induced corona streamers starts about 25-55 ns after the laser pulse. Moreover, the laser pulse itself can have a jitter which can be meaningful when the time resolution of nanosecond order is considered. Taking into account of these time delay characteristics for streamer inception, the technique based on Boxcar scanning was applied for the observation of the DC streamer corona development between the electrodes. Figure 7 shows the time evolution of the laser ( $\lambda = 281$  nm, pulse energy: 2 mJ) induced DC positive corona streamers. The focused laser beam was placed 1mm apart from the tip of the hollow electrode in order to reduce the time delay between the laser incidence and the streamer inception. The exposure time of the ICCD camera was 5 ns. The number in each image indicates the time (in ns) of opening the gate of ICCD camera in respect to the beginning of the streamer current waveform (D-S in Figure 2). The images were selected to be representative of the typical time evolution. Therefore, one should remember that each image shows different streamers. However, we confirmed that the streamers are quite reproducible. The bright spots in these images are the traces of the streamer heads. On the contrary, the streamer channels behind the streamer heads are dark, and thus invisible. However, an optical emission with two branches is seen around the tube tip over the life-time of the corona streamers. The nature of this optical emission is not clear at this stage. The streamer heads bridged the gap after about 120 ns. However, the late stages of streamers were still observed after

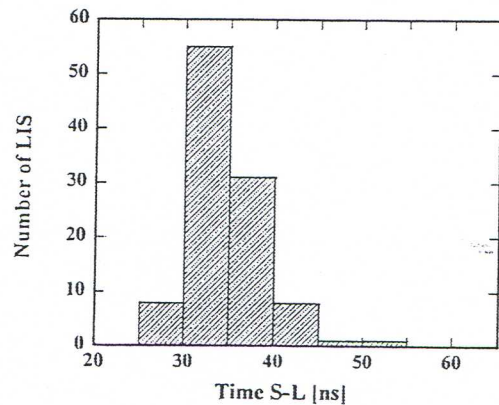


**Figure 6.** The distribution of the time delay (S-L in Figure 2) of UV laser (281 nm)-induced streamer in respect to the laser pulse. 'LIS' indicates the laser-induced streamers.

that time, as shown in Figures 7(k)-(n). The streamers last about 350ns and then disappear (Figure 7(p)).

It is seen from Figure 7 that the DC positive corona takes the form of a number of streamer heads, moving simultaneously through the gas. The number of heads increases during the propagation, which corresponds to the branching shown in Figure 3. Since the exposure time was 5 ns, each image shows the pathway the streamer head passed during 5 ns. The shape of the streamer head could not be resolved in this experiment; for that a much shorter exposure time and higher resolution of the image is needed. The arrival time of streamers at the grounded electrode coincides with the peak of streamer current waveform. We also found that the time resolved streamer structure induced by the KrF laser ( $\lambda = 248$  nm, pulse energy: 200 mJ) is similar to that induced by the dye laser with SHG ( $\lambda = 281$  nm, Figure 7).

The time evolution of the DC positive corona streamers makes the determination of the propagation velocity of the streamer head possible. The velocity ( $v$ ) of the streamer head can be calculated as a

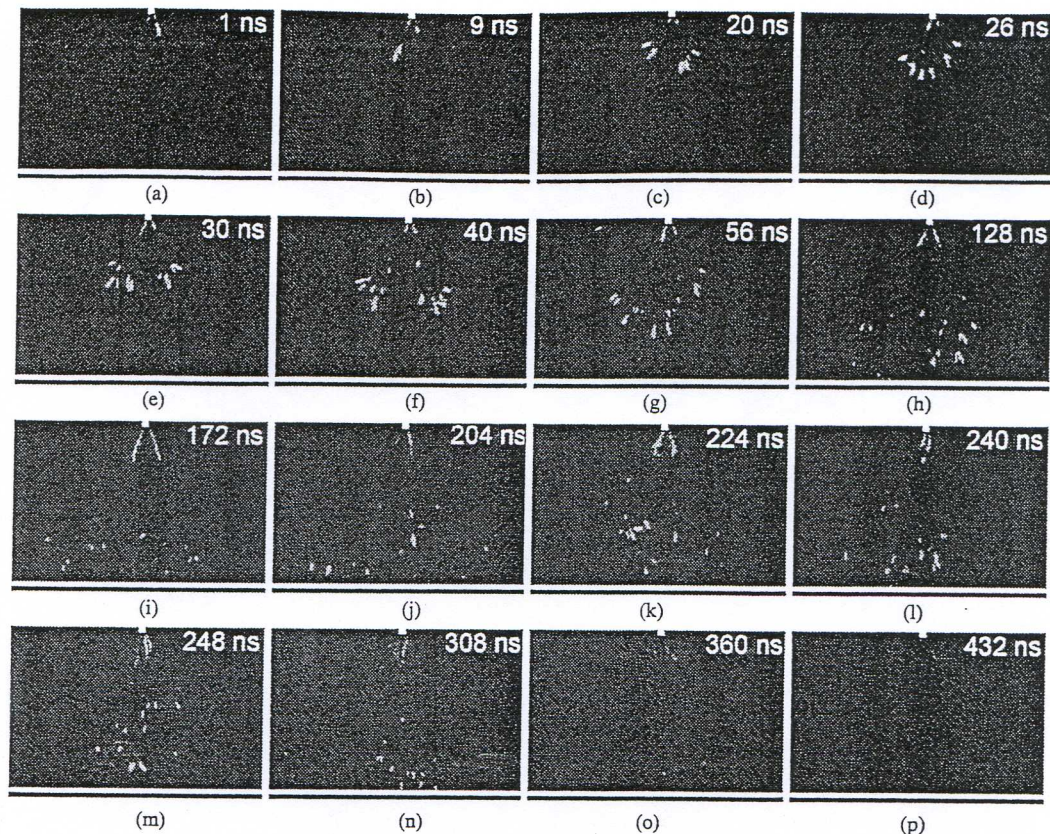


Figure 7. Time evolution of positive streamers induced by a single UV laser (281 nm) pulse in air. Gate time of ICCD camera: 5 ns. Gain of ICCD camera: 7. Number in the image indicates the time of opening the gate of ICCD camera in respect to the beginning of streamer current waveform (D-S in Figure 2). Applied voltage: 26 kV.

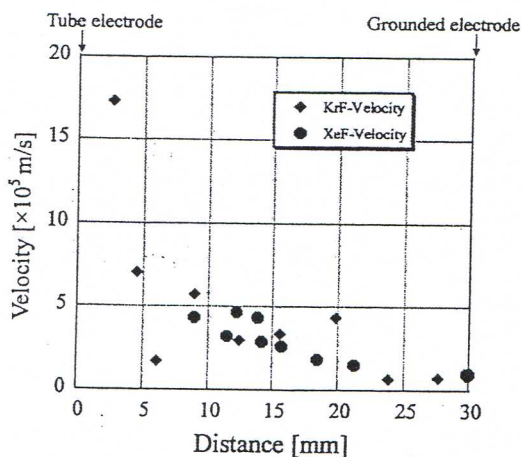


Figure 8. The streamer head propagation velocity along the electrode gap for UV laser (281 nm) and KrF laser (248 nm) induced streamers. Electrode gap: 3 cm, Applied voltage: 26 kV.

function of the distance from the tube electrode by the following equation:

$$v = \frac{\Delta x}{\Delta t} \quad (1)$$

where  $\Delta x$  is the distance between the streamer heads using the two consecutive streamer images and  $\Delta t$  is

the time interval between these images. Figure 8 shows the streamer head velocity as a function of position of the consecutive streamer heads in the electrode gap. It can be seen that the velocity of the streamer head decreases with increasing distance from the tube electrode and becomes constant near the grounded electrode. The velocity of the streamer head is higher than  $5 \times 10^5$  m/s near the tube electrode and it decreases down to about  $1 \times 10^5$  m/s near the grounded electrode. As the arrival time of streamers at the grounded electrode corresponds to the peak of streamer current waveform, we considered that the velocity for regular streamers is of the same order with that of the laser-induced streamers. The average velocity ( $2.5 \times 10^5$  m/s) is in a good agreement with the value of reported in (16). The velocity of DC streamer head is almost equal to that of the pulsed streamers (15) but is an order of magnitude lower than that of pulsed streamers (17, 29). In addition, the peak current of DC corona streamer is three-order of magnitude lower than that of the pulsed streamers at the similar peak applied voltage (15, 17, 18). The characteristics of DC streamers including the laser-induced streamers compared to

**Table 1.** Characteristic parameters of streamers in air (comparison between positive DC and pulsed coronas)

	DC corona (present study)	Pulsed corona
pulse repetition rate	1-10 kHz for one tube electrode	typical order: 1-100 pulses/s
current width	about 350 ns	about 50 ns <sup>(15)</sup> , 100 ns <sup>(17)</sup>
peak current	10-200 mA	8A <sup>(15)</sup> , 40-105A <sup>(17)</sup>
streamer velocity	$1 \times 10^5$ - $10 \times 10^5$ m/s*	$3 \times 10^5$ - $1.2 \times 10^6$ m/s <sup>(15)</sup> $1.8 \times 10^6$ - $3.3 \times 10^6$ m/s <sup>(17)</sup> $1 \times 10^5$ - $3 \times 10^6$ m/s <sup>(29)</sup>
streamer diameter	100-200 $\mu$ m	200 $\mu$ m <sup>(13)-(15)</sup> , ~ 1.2 mm <sup>(18)</sup> , 8 mm <sup>(29)</sup>
branching distance	about 0.5 - 2 cm	3 mm <sup>(29)</sup>
branching angle	about 40 degree in average	

\*The streamer velocity was determined using the data for the laser-induced streamers.

the pulsed streamers are summarized in Table 1. It is found that DC corona streamer and pulsed corona streamer are different from the view point of the discharge current and streamer structure.

### Conclusions

DC positive corona streamers in the tube-to-plane electrode configuration with a 3 cm gap in air were investigated. The time evolution of the streamers propagation along the electrode gap was visualized with the temporal resolution of 5 ns. To achieve this resolution the UV laser (281 nm)/KrF excimer laser (248 nm) were used to generate the streamers. The features of the regular streamers and the laser-induced streamers such as streamer number, length, diameter and branching were observed from three directions, perpendicular to each other.

It was observed that the laser-induced streamers were similar to the regular DC corona streamers. Therefore, the time evolution measurements of the laser-induced streamers were useful to investigate the streamer features of the DC regular streamers.

The velocity of the streamer head propagation was observed to be higher than  $5 \times 10^5$  m/s near the stressed electrode. It decreases to  $1 \times 10^5$  m/s near the grounded electrode.

About 120 ns after the streamer current start, the streamer head reached the grounded electrode and the discharge current pulse reaches the maximum in its waveform. The images showing the later stages of the streamer evolution was also recorded. The duration of current waveform coincides with the period of streamer evolution. The more precise measurements of the streamer head are necessary to find out the details of DC corona streamer morphology.

### Acknowledgement

This work was partially sponsored by Japan Society for Promotion of Science.

### References

- (1) Loeb, L. B. *Electrical Coronas*, Univ. of California Press, 1965.
- (2) Nasser, E. *Fundamentals of Gaseous Ionization and Plasma Electronics*; Wiley-Interscience: 1971.
- (3) Meek, J. M. *Electrical Breakdown of Gases*; Wiley Interscience: 1978.
- (4) Raizer, Y. P. *Gas Discharges Physics*, Springer: Berlin, 1991.
- (5) Bazelian, E. M.; Raizer, Y. P. *Spark Discharge*, MFTI, Moscow, 1997. (in Russian).
- (6) Vercammen, K. L. L.; Berezin, A. A.; Lox, F.; Chang, J. S. *J. Adv. Oxid. Technol.* **1997**, *2*, 312-329.
- (7) Manheimer, W.; Sugiyama, L. E.; Stix, Th.H., Eds., *Plasma Science and the Environ.*, AIP Press: 1997.
- (8) Hammer, T. *Contrib. Plasma Phys.* **1999**, *39*, 441-462.
- (9) Urashima, K.; Chang, J. S. *IEEE Trans. Dielectrics and Electrical Insulation* **2000**, *7*, 602-614.
- (10) Van Veldhuizen, E. M., Ed. *Electrical Discharges for Environmental Purposes: Fundamentals and Applications*; Nova Science Publishers, Inc.: 2000.
- (11) Chang, J. S. *Science and Technology of Advanced Materials* **2001**, *2*, 571-576.
- (12) Chang, J. S. *J. of Electrostatics* **2003**, *57*, 273-291.
- (13) Dyakonov, M. I.; Kachorovskii, V. Yu. *Sov. Phys. JETP*, **1988**, *94*, 321-332. (in Russian).
- (14) Kulikovskiy, A. A.; *J. Phys. D: Appl. Phys.* **1995**, *28*, 2483-2493.

- (15) Van Veldhuizen, E. M.; Rutgers, W. R. *J. Phys. D: Appl. Phys.* **2002**, *35*, 2169-2179.
- (16) Yan, K.; Yamamoto, S.; Kanazawa, S.; Ohkubo, T.; Nomoto, Y.; Chang, J. S. *J. of Electrostatics* **1999**, *46*, 207-219.
- (17) Namihira, T.; Wang, D.; Katsuki, S.; Hackam, R.; Akiyama, H. *IEEE Plasma Sci.* **2003**, *31*, 1091-1094.
- (18) Ono, R.; Oda, T. *J. Phys. D: Appl. Phys.* **2003**, *36*, 1952-1958.
- (19) Van Veldhuizen, E. M.; Baede, A. H. F. M.; Hayashi, D.; Rutgers, W. R. In *Proce. APP Spring Meeting*, Bad Honnef: Germany, 2001; pp 231-4.
- (20) Valette, N. *Internal Report EPG*, Eindhoven University of Technology, 2001.
- (21) Van Veldhuizen, E. M.; Kemps, P. C. M.; Rutgers, W. R. *IEEE Plasma Sci.* **2002**, *30*, 162-163.
- (22) Mizeraczyk, J.; Ohkubo, T.; Kanazawa, S.; Nomoto, Y. In *Proceedings of 1999 Annual Meeting of the Institute of Electrostatics Japan* Tsudanuma: Japan, 1999; pp 231-234.
- (23) Mizeraczyk, J.; Ohkubo, T.; Kanazawa, S.; Nomoto, Y.; Kawasaki, T.; Kocik, M. In *Laser Technology VI: Applications*, Woliński, W. L.; Jankiewicz, Z. Eds., In *Proc. of SPIE*, 2000, 4238, pp 242-245.
- (24) Ohkubo, T.; Ito, T.; Shuto, Y.; Akamine, S.; Kanazawa, S.; Nomoto, Y.; Mizeraczyk, J. *J. Adv. Oxid. Technol.* **2002**, *5*, 129-134.
- (25) Mizeraczyk, J.; Kanazawa, S.; Ohkubo, T. *J. Adv. Oxid. Technol.* **2004**, *7*, 129-134.
- (26) Izawa, Y., Yang, J. B., Nishijima, K., *Trans. Inst. Elect. Eng. Japan*, **2001**, *121-A*, 509-515. (in Japanese).
- (27) Ono, R.; Oda, T. *IEEE Trans. Ind. Applicat.* **2000**, *36*, 82-86.
- (28) Ershov, A.; Borysow, J. *J. Phys. D: Appl. Phys.* **1995**, *28*, 68-74.
- (29) Yi, W. J, Williams P. F. *J. Phys. D: Appl. Phys.* **2002**, *35*, 205-218.
- (30) Kanazawa, S.; Ito, T.; Shuto, Y.; Ohkubo, T.; Nomoto, Y.; Mizeraczyk, J. *J. of Electrostatics*, **2002**, *55*, 343-350.

Received for review September 16, 2004. Accepted January 18, 2005.